Photo-Crosslinked Side-Chain Liquid-Crystalline Elastomers for Microsystems

Antoni Sánchez-Ferrer,* Tamás Fischl, Mike Stubenrauch, Helmut Wurmus, Martin Hoffmann, Heino Finkelmann

Photo-crosslinkable side-chain liquid-crystalline polymers (LCPs) containing photoreactive benzophenone cores are synthesized in order to obtain their corresponding side-chain liquid-crystalline elastomers (LCEs). This strategic synthesis allows thin elastomeric films and their integration into microsystems for actuators and micromachines to be obtained. As an example of this principle, a gripper was developed. The position of its arms can be changed by applying voltages from 1.5 to 3.5 V at different rates. Small changes in the liquid-crystalline elastomer film cause strains of up to 150% in the microdevice and the capacity to move up to 400 times its own mass due to the nematic-to-isotropic transformation.

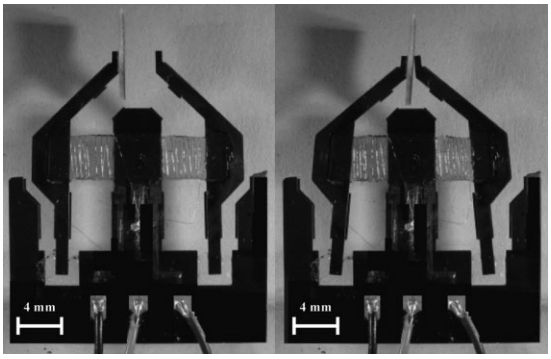

Introduction

Liquid-crystalline elastomers (LCEs) are the resulting combination of two properties: order, coming from the liquid crystal phase, and flexibility, from the rubber elasticity. The potential of these materials makes them interesting for microengineering, where their integration can induce the movement of a reduced volume engine. Temperature,[1] voltage,[2] or light[3,4] are driving forces than can produce such movements by inducing change of order in the liquid-crystalline structure.

A. Sánchez-Ferrer
University of Fribourg, Physics Department, Polymer Physics Group, Chemin du Musée, 3, 1700 Fribourg, Switzerland
T. Fischl, M. Stubenrauch, H. Wurmus, M. Hoffmann
Technische Universität Ilmenau, Institut für Mikro- und Nanotechnologien, FG Mikromechanische Systeme, Max-Plank-Ring 14, 98684 Ilmenau, Germany
A. Sánchez-Ferrer, H. Finkelmann
Albert-Ludwigs-Universität, Institut für Makromolekulare Chemie, Stefan-Meier-Str. 31, 79104 Freiburg, Germany
Fax: (+41) (0) 26 300 97 47; E-mail: antonio.sanchez-ferrer@unifr.ch

In this paper, the synthesis of photo-crosslinkable side-chain liquid-crystalline polymers (LCPs) and their corresponding photo-crosslinked side-chain LCEs is presented. LCPs with photo-crosslinkable units (benzophenone molecules) were synthesized and their oriented films photo-crosslinked. An option for the temperature–voltage control of LCEs is the introduction of conductive carbon black particles, but these systems are not suitable due to their huge absorption that prevents photo-crosslinking.[2]

The actuator materials consist of thin films of LCEs with good mechanical properties, which can be integrated into silicon-based Microsystems[5] by a dry chemical etching process (oxide etching and silicon etching). The resulting device shows temperature-controlled motions. New machines can be constructed, where movements are produced by mechanical forces caused by changes in temperature[6] (due to external voltage or light).

Experimental Part

Apparatus and Techniques

Mesophases were analyzed using a Leitz Ortholux II-POL-BK polarized light optical microscope, equipped with a Nikon Coolpix 990 digital camera. The thermal analysis was done using a Mettler

DOI: 10.1002/macp.200900308

FP82 hot stage with a Mettler FP80 central processor. The phase transformation behavior was investigated by differential scanning calorimetry (DSC) measurements using a PerkinElmer Pyris 1 differential scanning calorimeter at a heating rate of $10\,K \cdot min^{-1}$ and under N_2 atmosphere. The glass transition temperature (T_g) was determined by the half-vitrification temperature ($1/2\Delta C_p$). The liquid-crystalline-to-isotropic phase transformation temperature (T_{NI}) was determined from temperatures of the maxima of the heat flow. The changes in the heat capacity (ΔC_p) and in the latent heat (ΔH_{NI}) were calculated from the thermograms. Samples were characterized by ^1H and ^{13}C NMR spectroscopy with a Bruker ARX300 (300 MHz for ^1H and 75 MHz for ^{13}C) spectrometer. The infrared (FT-IR) spectra were recorded with a Nicolet 5DXC spectrometer using NaCl windows. The orientation of side-chain polymers was done using a Bruker B-MNC5 magnet at 11.1 T and the temperature was controlled by a Haake-F6 thermostat. Photocrosslinking processes of side-chain LCPs with benzophenone moieties were carried out to obtain side-chain LCEs, using a Philips HPL-R 400 W high-pressure mercury lamp, which was in a self-constructed lamp housing with ventilators to keep the temperature constant. In order to irradiate with only UV-light, an Edmund Optics NT54-516 IR-cut-off filter (50 mm^2, 3.3 mm) and a LINOS UG11 UV-transmitting glass filter (360 nm, 50 mm diameter, 3 mm thickness) were used. Thin layers of side-chain polymers were obtained by using a glass wafer with a sacrificial layer of 5% PEOX in ethanol, where a solution of 10% of polymer in DCM was spin-coated using a Specialty Coating Systems P6700 spin-coater at 3 000 rpm. The purification of all polymers by re-precipitation was carried out using a Heraeus Biofuge Primo centrifuge at 6 000 rpm. The thicknesses of all elastomeric samples were measured using a Mitutoyo PAT460176 (10 μm to 10 mm) thickness gauge.

Monomers

The low molecular weight host liquid crystal (SCM) was synthesized according to previous works.[7–9] The benzophenone derivative (SCPC) was obtained using Mitsubonu conditions.[10,11] In a 250 mL round-bottomed flask, 10.0 g (50 mmol) of 4-hidroxybenzophenone, and 14.6 g (56 mmol) of triphenylphosphine (PPh_3) were placed, and 50 mL of anhydrous THF were added. The system was magnetically stirred and purged with nitrogen for 15 min. Then 8.6 g (50 mmol) of undec-10-en-1-ol were added. In the next step, the solution was magnetically stirred under nitrogen, and 11.2 g (56 mmol) of diisopropyl aza-1,2-dicarboxylate (DiPAD) was added. The reaction was stirred at room temperature and controlled by TLC (SiO_2, CH_2Cl_2). On disappearance of the starting phenol derivative (after about 8 h), the reaction was complete. Then hexane/AcOEt (5:1 v/v) was added and the white solid, triphenylphosphine oxide, was precipitated. The solution was filtered and evaporated. The residue was purified through a silica gel column ($CHCl_3$); yield: 17.4 g (98%); ^1H NMR (300 MHz, $CDCl_3$): $\delta = 7.80$ (2H, d, *o*-Ar, $J = 8.7$ Hz), 7.72 (2H, dd, *o*-Ar′, $J = 6.9$ Hz, $J = 1.6$ Hz), 7.54 (1H, tt, *p*-Ar′, $J = 7.3$ Hz, $J = 1.6$ Hz), 7.44 (2H, td, m-Ar′, $J = 7.5$ Hz, $J = 6.9$ Hz), 6.92 (2H, d, *m*-Ar, $J = 9.0$ Hz), 5.79 (1H, ddt, C*H*=CH_2, $J = 17.1$ Hz, $J = 10.2$ Hz, $J = 6.7$ Hz), 4.97 (1H, ddt, *cis*-CH=CH_2, $J = 17.1$ Hz, $J = 2.2$ Hz, $J = 1.6$ Hz), 4.92 (1H, ddt, *trans*-CH=CH_2, $J = 10.2$ Hz, $J = 2.2$ Hz, $J = 1.2$ Hz), 4.01 (2H, t, CH_2OAr, $J = 6.6$ Hz), 2.01 (2H, tt, CH_2, $J = 7.5$ Hz, $J = 6.7$ Hz), 1.79 (2H, tt, CH_2, $J = 7.6$ Hz, $J = 6.9$ Hz), 1.52–1.38 (2H, m, CH_2), 1.38–1.22 (10H, m, CH_2) ppm; ^{13}C NMR (75 MHz, $CDCl_3$): $\delta = 195.7$ (C=O), 162.8 (ArCO), 139.1 (*C*H=CH_2), 138.2 (Ar′), 132.5 (2C, *o*-Ar′H), 131.8 (*p*-Ar′H), 129.7 (Ar), 129.6 (2C, *m*-Ar′H), 128.1 (2C, *m*-ArH), 114.0 (CH=*C*H_2), 113.9 (2C, *m*-ArH), 68.2 (CH_2OAr), 33.7 (CH_2), 29.4 (CH_2), 29.3 (CH_2), 29.2 (CH_2), 29.0 (2C, CH_2), 28.8 (CH_2), 25.9 (CH_2) ppm; FT-IR (NaCl): 1 652 (st, C=O), 1 600 (st, C=CH_2), 1 255 (st, C–O) cm^{-1}; m.p.: 48 °C.

Photo-Crosslinkable Side-Chain Liquid-Crystalline Polymers (LCPs)

In a 10 mL round-bottomed flask, 4-methoxyphenyl 4-(but-3-en-1-yloxy)benzoate (SCM) (*x* mmol), 4-(undec-10-en-1-yloxy)benzophenone (SCPC) (*z* mmol), and polymethylhydrosiloxane (PMHS) ($x + z$ mmol), $\overline{DP} = 259$ were placed. 1 mL of thiophene free toluene and 20 μL of 1%-Pt cyclooctadiene platinum (II) chloride [$Pt(COD)Cl_2$] in DCM were then added. The mixture was heated at 60 °C for 2 h, and the reaction was controlled by FT-IR. When the vibration band at 2 100 cm^{-1} (Si–H) disappeared (after 18 h), the reaction was complete. The solvent was evaporated and the viscous product was dissolved in THF. The solution was poured in cold methanol to precipitate the polymer and centrifuged at 6 000 rpm for 3 min. This process was repeated three times and the solvent was then evaporated. The polymer was freeze-dried for 1 d.

Liquid-crystalline polymer (LCP-10), ^1H NMR (300 MHz, $CDCl_3$): $\delta = 8.16–7.89$ (2H, m, *o*-Ar), 7.89–7.62, 7.58–7.34, 7.14–6.93, 6.93–6.64, 5.05–3.82, 3.82–3.58, 1.90–1.65, 1.65–1.43, 1.43–1.08, 0.74–0.45, 0.27–0.01 (3H, m, CH_3Si) ppm; FT-IR (NaCl): 1 734 (st, C=O), 1 651 (st, C=O), 1 267 (st, C–O and Si–CH_3), 1 068 (st, Si–O), 847 and 764 (st, Si–CH_3) cm^{-1}; yield = 94%; DSC ($10\,K \cdot min^{-1}$, N_2): g 10 ($0.4\,J \cdot g^{-1} \cdot K^{-1}$) N 59 ($0.9\,J \cdot g^{-1}$) I °C.

Liquid-crystalline polymer (LCP-5), ^1H NMR (300 MHz, $CDCl_3$): $\delta = 8.16–7.89$ (2H, m, *o*-Ar), 7.89–7.62, 7.58–7.34, 7.14–6.93, 6.93–6.64, 5.05–3.82, 3.82–3.58, 1.90–1.65, 1.65–1.43, 1.43–1.08, 0.74–0.45, 0.27–0.01 (3H, m, CH_3Si) ppm; FT-IR (NaCl): 1 732 (st, C=O), 1 654 (st, C=O), 1 259 (st, C–O and Si–CH_3), 1 072 (st, Si–O), 845 and 765 (st, Si–CH_3) cm^{-1}; yield = 95%; DSC ($10\,K \cdot min^{-1}$, N_2): g 10 ($0.4\,J \cdot g^{-1} \cdot K^{-1}$) N 67 ($1.0\,J \cdot g^{-1}$) I °C.

Photo-Crosslinked Side-Chain Liquid-Crystalline Elastomers (LCEs)

A solution of LCP (10%) in dichloromethane (DCM) was placed onto a glass wafer containing a water-soluble polymer layer [5% of PEOX (poly-2-ethyl-2-oxazoline, $\overline{M}_w = 50\,000\,g\,mol^{-1}$) in ethanol] and the solvent was evaporated. A homogeneous thin film was obtained on heating the layer above the clearing temperature and using the spin-coating technique at 3 000 rpm or by evaporation. The sample was placed under a magnetic field of 11 T, below the clearing temperature, for three days in order to obtain oriented polymers. Afterwards, the oriented monodomain polymer film was photo-crosslinked by irradiating the sample from both sides for 1 h using UV-light. The elastomer film was removed by dissolving the sacrificial layer (PEOX) with water. Polydomain samples were obtained without the use of a magnetic field and further photo-crosslinking.

Macromolecular Journals
DOI: 10.1002/macp.200900308

Liquid-crystalline elastomer (LCE-10), DSC (10 K · min^{-1}, N_2): g 10 (0.4 J · g^{-1} · K^{-1}) N 53 (0.8 J · g^{-1}) I °C.

Liquid-crystalline elastomer (LCE-5), DSC (10 K · min^{-1}, N_2): g 10 (0.4 J · g^{-1} · K^{-1}) N 65 (0.8 J · g^{-1}) I °C.

Results and Discussion

Synthesis of Side-Chain Liquid-Crystalline Polymers (LCPs) and Elastomers (LCEs)

Due to the easy chemistry and orientation of the linear polymers by external fields, two different LCPs were synthesized to obtain thin LCE films: one polymer containing 10 mol-% (LCP-10) and another with 5 mol-% (LCP-5) of benzophenone units (Scheme 1). The cross-linker percentages were chosen for the study of the mechanical behavior of the corresponding elastomers with elastic moduli in the range of 100 kPa, which is a typical range for rubbers, and which can be obtained by a photo-crosslinking process, where the benzophenone moiety creates the polymer network and the elastomers are attached to the surface of the machines.

Liquid-crystalline polymers (LCPs) are easily synthesized by attaching the mesogens to a siloxane polymer backbone. The mesogens that contain a double bond are connected to the silicon atom via the hydrosilylation reaction, (the addition of Si—H bonds from a hydrosilane to double bonds like C=C in olefins).[12–15] Likewise, one can also introduce photoreactive moieties, i.e., benzophenone derivatives, which react then, under UV-irradiation with any aliphatic chain and crosslink two polymer chains. In this way, one can obtain elastomers of a well-defined thickness after orienting and crosslinking the polymer chains.

Oriented LCEs with well-defined thickness were synthesized for their integration into microsystems and the construction of microdevices. After obtaining a thin polymer film, the sample was photo-crosslinked[16] and a thin elastomer was obtained.[17,18] The photo-crosslinking process for obtaining LCEs is also shown in Scheme 1.

Solutions of LCP (10%) in DCM were prepared, and thin polymer films were obtained either by spin coating, or by evaporation. It is also possible to obtain oriented elastomer films (monodomains) by orienting the polymer films under electric or magnetic fields and later photo-crosslinking the polymer chains. First, the polymer film was oriented over a period of three days below the clearing temperature and at a magnetic field strength of 11 T, and photo-crosslinked using UV light (Philips HPL-R 400 W high-pressure mercury lamp with an Edmund Optics NT54-516 IR-cut-off filter and a LINOS UG11 UV-transmitting glass filter). The resulting free-standing elastomer was a monodomain sample.

Characterization of Side-Chain Liquid-Crystalline Polymers (LCPs) and Elastomers (LCEs)

The liquid-crystalline-to-isotropic transition temperatures and mesophases of LCPs were measured by POM and DSC experiments.

Both samples showed a nematic phase, detected from the values of the latent heat (ΔH_{NI}) around 1 J · g^{-1}, and textures under the microscope, and had the same T_g at 10 °C. The difference in the clearing temperature, T_{NI} at 59 for LCP-10 and 67 °C for LCP-5, can be explained by the different concentrations in benzophenone moieties (SCPC), that did not change the phase structure but for the sample with 10 mol-% of photo-crosslinker, reduced the T_{NI} due to its non-liquid-crystalline behavior.

In order to investigate the liquid-crystalline phases and their orientation, LCEs were characterized by DSC, polarized optical microscopy (POM), and X-ray diffractometry (XRD). The change in length of the elastomeric samples as a function of temperature was carried out by themoelastic experiments.

Differential scanning calorimetry (DSC) measurements showed T_g around 10 °C and latent heats (ΔH_{NI}) of less than 1 J · g^{-1} for both samples. The nematic-to-isotropic transition temperatures (T_{NI}) were around 53 °C for elastomer films with 10 mol-% crosslinking density (LCE-10), and higher (65 °C) for the sample with 5 mol-% crosslinking density (LCE-5). Thus the presence of more crosslinking points in the elastomers, lowered the transition tempera-

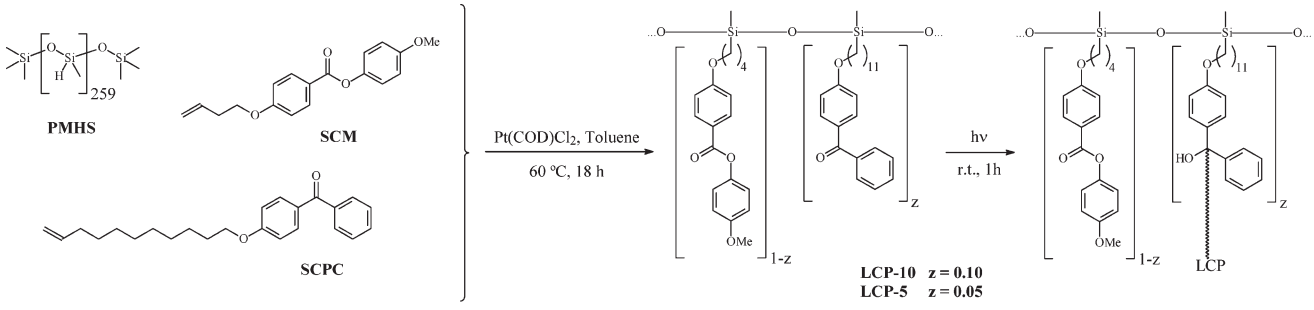

Scheme 1. Synthetic procedure for LCPs and LCEs.

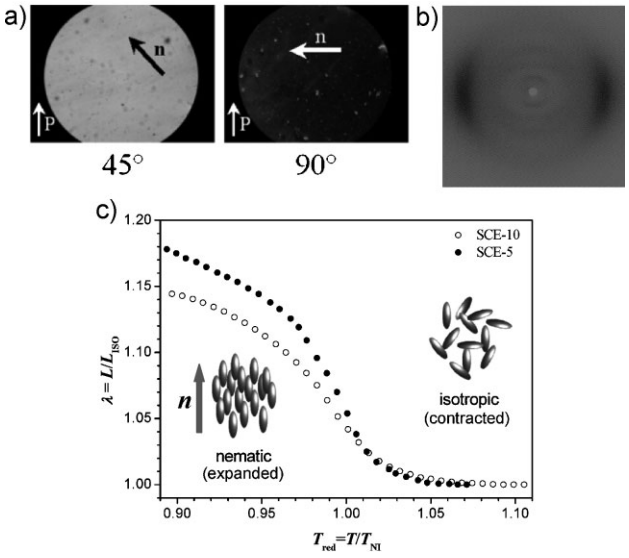

Figure 1. a) POM pictures of a monodomain from the sample LCE-10 of 20 μm thickness oriented over 3 d at 11 T and below 53 °C after photo-crosslinking. b) X-ray pattern of a sandwich sample of a LCE at room temperature ($S = 0.59$). c) Uniaxial thermal expansion as a function of the temperature for both elastomers.

ture of the resulting LCE due to the non-liquid-crystallinity of the crosslinker.

To analyze the quality of the uniform director orientation, POM experiments on oriented samples or monodomains were performed. With this technique, the orientation of the sample can be easily determined. These experiments revealed a maximum in the intensity of light passing through the film at 45° and 135° with respect to the analyzer of the microscope, and a minimum where samples were at 90° and 180°. In Figure 1(a), the change in the sample's intensity is shown, a proof that the mesogens have planar orientation with the director *n* parallel to the glass surface, but more importantly indicating that the mesogens are aligned along with the direction parallel to the applied magnetic field.

To analyze the order parameter, X-ray experiments on aligned samples revealed the nematic phase of the elastomers while oriented, as it can be observed from the two reflections in the wide-angle region [Figure 1(b)]. From the azimuthal intensity distribution, the nematic order parameter was calculated and was for all samples around $S = 0.60$.

The thermal behavior of the samples as a function of temperature was determined from the thermoelastic measurements [Figure 1(c)], and showed that the sample with 5 mol-% of crosslinking points, LCE-5, expands up to 18% of its isotropic dimension, while the sample with 10 mol-% of benzophenone units, LCE-10, only up to 15%. The cross-linking density of the samples explains this difference, where one would expect higher expansions for the lowest cross-linked elastomer. LCEs synthesized by the two-step crosslinking technique[7–8] showed changes in length up to 60%. The main reason for the low expansion in photo-crosslinked LCEs is due to the orientation of the mesogenic units and the low coupling with the polymer backbone, a process much more difficult than the induced orientation of the mesogens when the polymer backbones are stretched.

Integration of Liquid-Crystalline Elastomers in Microsystems

Besides the evaluation of the mechanical properties and the long-term stability of the materials, it was necessary to show compatibility with standard materials used for Microsystems Technology, such as silicon or glass substrates, and the process to manufacture the system. A solution of LCP in DCM was deposited on silicon substrates and exposed to strong electric or magnetic fields of 300 $kV \cdot m^{-1}$ or 11 T, respectively, in order to orient the LCPs. Then, using a mask, the polymer was exposed to UV-light for photo-crosslinking. To obtain the free-standing elastomer membranes, advanced silicon etching (ASE®) was used.[19] This class of integrated smart materials shows a reversible change of shape when heated (Figure 2).

Thin films are available to be used for the build-up of microdevices due to their ease of integration and mechanical properties. To test the compatibility with microtechnology, an actuator was designed as an example of an application model for utilizing elastomers as molecular motors.

The arm structure shown in Figure 3 is the first microtechnological application of such LCE actuators achieved through microintegration. Once the maximum strain of the LCE (LCE-10) is known, the construction of the micromachine can be designed such as to obtain a single arm movement of $d = 1.36$ mm from a change in length of the LCE of $L\text{-}L_{ISO} = 0.55$ mm, where L is the length of the

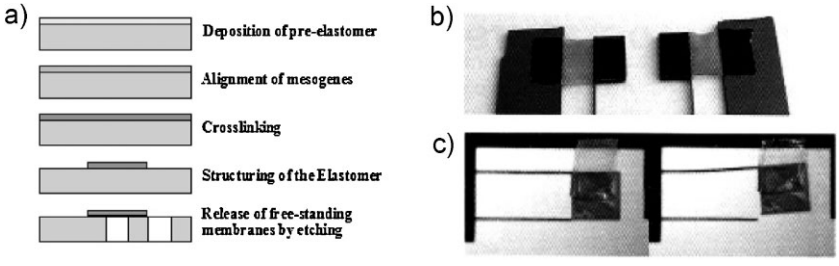

Figure 2. a) Required process steps for monolithic integration. b) Free-standing elastomer membranes released by ASE®. c) Deformation of a silicon structure due to the shrinking of LCE.

Macromolecular Journals
DOI: 10.1002/macp.200900308

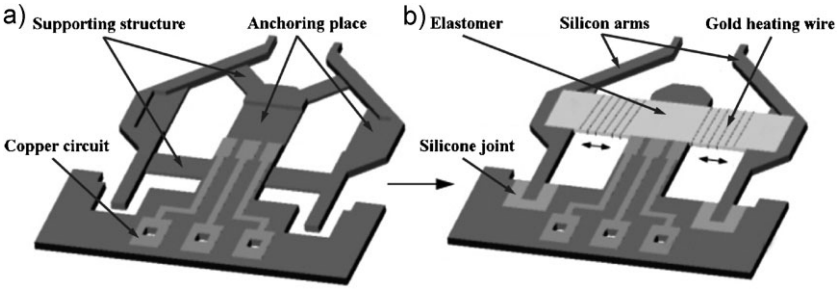

Figure 3. Detail of the LCE actuator and its components: a) silicon carrier during batch manufacturing, b) elastomer mounted onto the finished gripper mechanism (elastomer dimensions: 16 × 4 × 0.030 mm³; arm length: 20 mm; frame dimensions: 22 × 25 mm²).

elastomer in the nematic phase at 25 °C and L_{ISO} the minimum length in the istropic state. This movement corresponds to a total strain $\varepsilon = d/(L\text{-}L_{ISO}) = 2.46$ (146%) in the microdevice, which is equal to the rotation ratio between the arm radius $R = 20.35$ mm and the elastomer radius $r = 8.32$ mm ($R/r = 2.45$) when they rotate by an angle of 4° due to the contraction of the elastomer ($\lambda = L/L_{ISO} = 1.16$ or 16%) [see details in Figure 4(a)].

An electric voltage of 1.5 to 3.5 V is applied which produces a temperature increase in the surroundings of the elastomer strip and a strain leading to the contraction of the LCE, which in turn controls the movement of the arms of the micromachine. Experiments on the microactuator showed a uniaxial deformation of up to $\varepsilon = 150\%$, actuator stress values of 60 kPa and a tensile strength of 0.6 MPa.

In order to produce the electric terminals, the silicon wafer was first masked and metallized with copper by the lift-off process. Then both sides underwent two dry chemical etching processes (RIE → oxide etching, ASE® → silicon etching) to create the arm structures and areas for the joints and LCE film. Following this procedure, the LCE film was applied onto the anchoring point on the etched silicon wafer in two ways: the silicon surface and the actuator film can be activated with oxygen plasma, which gives better adhesion between the two surfaces; or the actuator film can be directly embedded into the silicon.

To heat the LCE, 8 to 10 windings of gold wire (25 μm thick) were wounded around the film. The motion loss of the system, 10% of the thermal expansion of the film, λ, was minimized by using elastic silicone that filled the joint arms. By removing the thin supporting structures deliberately produced during the dry chemical etching process, laser cutting was applied to release the gripper arms. When the arms were cut free, they were linked to the silicon base structure only by elastic elements (silicone). Laser cutting offers the advantage that the elastic structures are subjected to neither mechanical stress nor any heat due to the good thermal conductivity of silicon.

Mechanical Testing of the Microactuator

The controlled heating induced by the voltage applied on the gold wires was monitored. When the controlled voltage was altered, the temperature around the actuator changed inducing a mechanical stress, which ultimately caused the movement of the arms. In Figure 4(b), the thermal contraction–expansion ($\lambda = L/L_{ISO}$) as function of the time for a fixed voltage rate is shown, as well as its evolution as a function of the variation of voltage. The chosen voltage was 2.7 V, since no differences at higher voltages were observed for the strain of the LCE. From these plots, the time at the

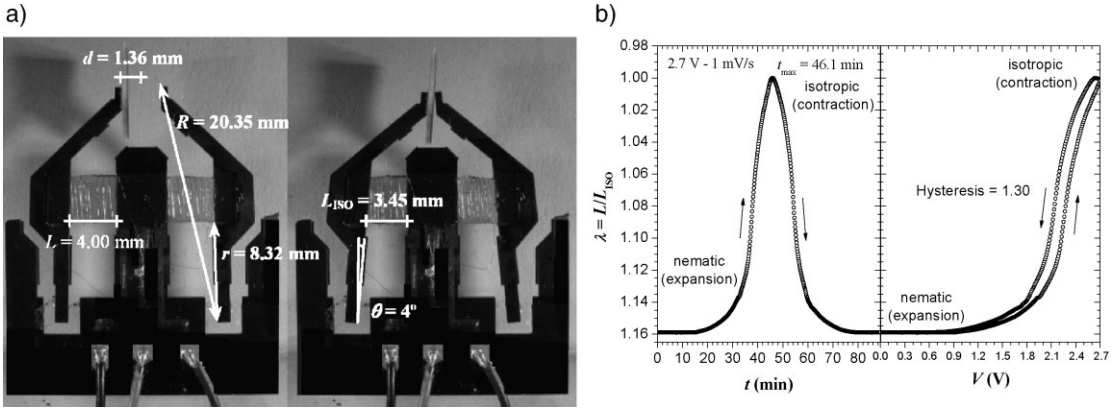

Figure 4. a) Open (left) and closed (right) liquid-crystalline elastomeric microgripper on applying an electrical power, where the nematic-to-isotropic transformation induces changes of the liquid-crystalline elastomer film length that causes the strain. b) Thermal contraction–expansion (λ) as function of the heating–cooling time (left) and as function of the variation of voltage (right) for the microgripper prepared with the sample LCE-10.

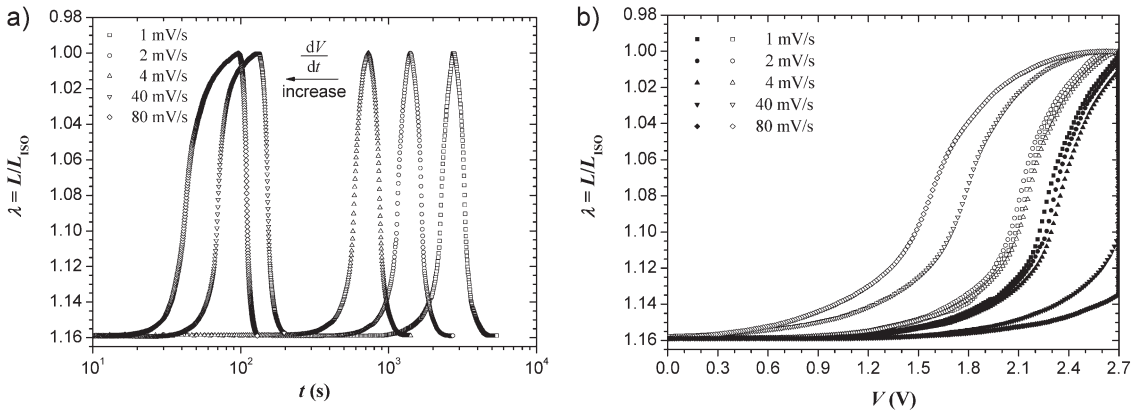

Figure 5. a) Thermal contraction–expansion (λ) versus time curves, and b) thermal contraction–expansion (λ) as a function of applied control voltage curves for the actuator at different voltage rates (filled symbols: heating processes; empty symbols: cooling processes).

maximum response, $\lambda = 16\%$, and the hysteresis, the ratio between the area under the cooling and heating curves, of the heating–cooling cycle, can be evaluated.

In Figure 5, the time response of the actuator at different voltage rates (dV/dt) is depicted, where the maxima can be evaluated. Fast and slow motions can be achieved with high precision in the movement of the arms by playing with the voltage rate. These curves show that the response time [Figure 5(a)] can be modulated from low voltage rates of $1\,mV \cdot s^{-1}$ ($t_{max} = 46.1$ min) to $80\,mV \cdot s^{-1}$ ($t_{max} = 1.6$ min), with an increased hysteresis factor ranging from 1.30 to 17.5 [Figure 5(b)]. All these data are collected in Table 1.

The extreme deformability of the LCE materials, as compared with piezoelectric materials, permits very large movements. So far only thermo-mechanical actuators have been considered. In the future, with only a small change to the microtechnology, it will be possible to adapt existing opto-mechanical LCEs for actuators that can be used in various applications such as pumps, valves, and switches. Electric frequencies of up to 0.15 Hz can be achieved. The response time to within ±5% of the final position is about 50 s. Such an actuator is suitable for slow, sensitive positioning and gripping movements.

Figure 6 resumes these experiments, showing the time to achieve the maximum response (t_{max}) and the hysteresis factor as a function of the voltage rate. The time response has a stretched exponential decay, while the hysteresis factor seems to follow a linear behavior. Experiments at a different voltage rate did adjust to the curves, showing that the time response and hysteresis can be predicted by the applied voltage rate.

In order to evaluate the efficiency of the system, the energy needed to increase the temperature from 25 °C (nematic phase) to 60 °C (isotropic phase) was calculated by considering a heat capacity of $C_p = 2\,J \cdot g^{-1} \cdot mol^{-1}$, already reported by ac and relaxation heat capacity measurements,[20]

Table 1. Time of response (t_{max}) and hysteresis factors for the heating–cooling cycles at different voltage rates.

dV/dt	t_{max}	Hysteresis
$mV \cdot s^{-1}$	min	
1	46.1	1.3
2	23.4	1.5
4	12.2	1.5
10	5.9	3.5
40	2.2	8.2
50	2.2	9.3
80	1.6	17.5

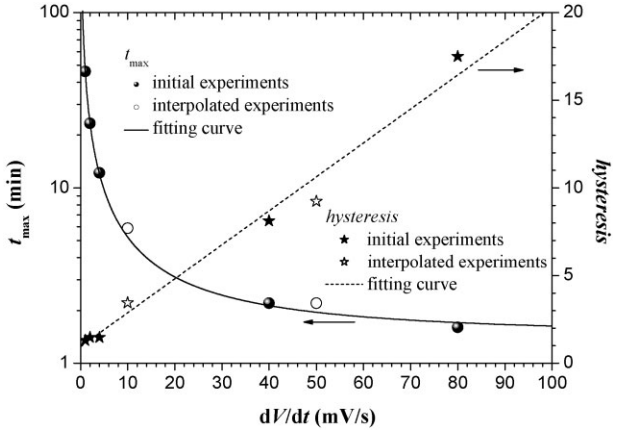

Figure 6. Maximum time response (circles) and hysteresis factor (stars) as function of the voltage rate (filled symbols: experiments are the initial experiments; empty symbols: interpolated experiments).

Macromol. Chem. Phys. **2009**, *210*, 1671–1677

DOI: 10.1002/macp.200900308

and the latent heat of the nematic-to-isotropic transition of $\Delta H_{NI} = 0.8\,J \cdot g^{-1}$. As a result, the transferred heat for the complete contraction of the LCE is $Q = 0.36$ J, energy used for the movement of the arm, and friction of the system. The applied electrical energy was calculated from the area under the curve V^2/R versus t, where V is the applied voltage as function of time, R the resistance of the gold wires, and t the time taken to reach the final voltage during the contraction or expansion of the elastomer. The corresponding electrical power was calculated by dividing the obtained energy by the total time. Thus, the values of the electrical power range from 0.2 W (at $1\,mV \cdot s^{-1}$) to 0.5 W (at $80\,mV \cdot s^{-1}$). The efficiency for the movement of the arm which requires a maximum force of $F = 21$ mN with a stress of $\sigma = 170$ kPa and strain of $\varepsilon = 150\%$ goes from 0.1% (at $1\,mV \cdot s^{-1}$) to 1% (at $80\,mV \cdot s^{-1}$). This level of efficiency can be explained by the loss of heat to the surroundings of the wires, viscosity of the polymer network, and the proximity of the initial temperature to the T_g of the LCE sample.

Conclusion

Liquid-crystalline elastomers (LCEs) are materials suitable for the application in Microsystems Technology, due to their good integration and their large strain values. LCPs were synthesized, oriented, and crosslinked, and thin side-chain LCEs were obtained which exhibit nematic phases. A microactuator prototype has been developed and manufactured, and its thermal controlled response analyzed at different voltage rates, showing that the principle can be applied for technological applications such as pumps, valves, and switches. Such actuators are suitable for slow, sensitive positioning, and gripping movements.

Further research will focus on developing materials exhibiting improved energy efficiency and faster changes in dimensions, with potential used in, e.g., artificial muscles.

Acknowledgements: The authors acknowledge financial support from the *Research Training Networks Functional Liquid-Crystalline Elastomers* (FULCE – HPRN-CT-2002-00169) and *Fonds der Chemischen Industrie*.

Received: June 22, 2009; Revised: July 22, 2009; Published online: September 22, 2009; DOI: 10.1002/macp.200900308

Keywords: actuator; elastomers; films; liquid crystal; microsystems; photo-crosslinking

[1] H. Wermter, H. Finkelmann, *e-Polymers* **2001**, no. 013.
[2] M. Chambers, B. Zalar, M. Remškar, S. Žumer, H. Finkelmann, *Appl. Phys. Lett.* **2006**, *89*, 243116.
[3] H. Finkelmann, E. Nishikawa, G. G. Pereira, M. Warner, *Phys. Rev. Lett.* **2001**, *87*, 015501.
[4] M. Camacho-López, H. Finkelmann, P. Palffy-Muhoray, M. Shelley, *Nat. Mater.* **2004**, *3*, 307.
[5] M. Bründel, M. Stubenrauch, H. Wurmus, A. Sánchez-Ferrer, *International Newsletter on Micro-Nano Integration* (MST-NEWS) **2004**, *4*, 38.
[6] T. Fischl, A. Albrecht, H. Wurmus, M. Hoffmann, M. Stubenrauch, A. Sánchez-Ferrer, *Kunststoffe* **2006**, *96*, 30.
[7] J. Küpfer, H. Finkelmann, *Macromol. Chem. Rapid Commun.* **1991**, *12*, 717.
[8] J. Küpfer, H. Finkelmann, *Macromol. Chem. Phys.* **1994**, *195*, 1353.
[9] H. Finkelmann, U. Kiechle, G. Rehage, *Mol. Cryst. Liq. Cryst.* **1983**, *94*, 343.
[10] M. Amaike, H. Kobayashi, K. Sakurai, S. Shinkai, *Supramol. Chem.* **2002**, *14*, 245.
[11] O. Mitsunobu, M. Wada, T. Sano, *J. Am. Chem. Soc.* **1972**, *94*, 679.
[12] B. Marciniec, *Comprehensive Handbook on Hydrosilylation*, Pergamon, Oxford 1992.
[13] J. Yoshida, K. Tamao, M. Takahashi, M. Kumada, *Tetrahedron Lett.* **1978**, *25*, 2161.
[14] W. Caseri, P. S. Pregosin, *Organometallics* **1988**, *7*, 1373.
[15] N. Sabourault, G. Mignani, A. Wagner, C. Mioskowski, *Org. Lett.* **2002**, *4*, 2117.
[16] C. E. Bell, A. K. Clark, D. F. Taber, O. D. Rodig, *Organic Chemistry Laboratory: Standard and Microscale Experiments*, Saunders College, New York 1996, p. 153.
[17] A. Komp, J. Rühe, H. Finkelmann, *Macromol. Rapid Commun.* **2005**, *26*, 813.
[18] J. Schmidtke, S. Kniesel, H. Finkelmann, *Macromolecules* **2005**, *38*, 1357.
[19] D. C. Duffy, J. C. McDonald, O. J. Schueller, G. M. Whitesides, *Anal. Chem.* **1998**, *70*, 4974.
[20] A. Lebar, Z. Kutnjak, S. Žumer, H. Finkelmann, A. Sánchez-Ferrer, B. Zalar, *Phys. Rev. Lett.* **2005**, *94*, 197801.